JOC The Journal of Organic Chemistry

pubs.acs.org/joc Article

Density Functional Theory Study of Mechanisms of [8 + 2] Cycloadditions of Dienylfurans/Dienylisobenzofurans with DMAD

Qi Cui, Yuanyuan Chen, James W. Herndon, and Zhi-Xiang Yu*

Cite This: J. Org. Chem. 2021, 86, 1419–1429 Read Online

ACCESS | Metrics & More | Article Recommendations | Supporting Information

ABSTRACT: The mechanisms of [8 + 2] cycloaddition reactions between dienylfurans/dienylisobenzofurans and the activated alkyne, DMAD (dimethyl acetylenedicarboxylate), have been investigated by DFT calculations. The former [8 + 2] reaction is stepwise, starting from attack of the diene substituent on furan, not the furyl moiety in dienylfurans, to DMAD to give a diradical intermediate, which then undergoes ring closure to form the second bond between DMAD and the furan moiety, generating the final [8 + 2] cycloadducts. In contrast, the latter [8 + 2] reaction starts from [4 + 2] cycloaddition of the diene in the furan ring of dienylisobenzofurans toward DMAD, followed by the rate-determining stepwise [1,5]-vinyl shift, forming the [8 + 2] products. The different mechanisms of [8 + 2] reactions are attributed to the facts that for dienylfurans, the reactive diene part is the diene substituent on furan, but in the case of dienylisobenzofurans, it is the diene in the furan ring (its reaction with DMAD to generate an aromatic benzene ring is the driving force for this regiochemistry). Consequently, the [8 + 2] reactions begin with the reaction of the most reactive part of tetraene (either the diene substituent on furan for dienylfurans or the diene in the furan ring for dienylisobenzofurans) with DMAD. FMO analysis and kinetic study have been carried out to gain more information of the reaction mechanisms. Two [8 + 2] reactions of dienylisobenzofurans with different substituents toward DMAD have also been further analyzed by DFT calculations in this paper.

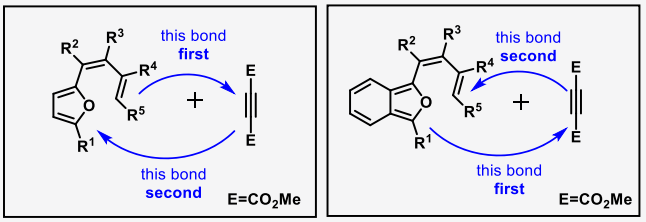

[8+2] Reactions in Different Pathways

INTRODUCTION

Since the seminal report of the [8 + 2] cycloaddition of heptafulvene and dimethyl acetylenedicarboxylate (DMAD) in 1960,[1] significant advances have been achieved by both synthetic and theoretical organic chemists in their search for other [8 + 2] cycloadditions.[2] However, most previously reported [8 + 2] cycloadditions are restricted to geometrically rigid tetraenes where carbons or heteroatoms at terminal positions one and eight of the tetraene are rigidly held in close proximity.[3] Successful [8 + 2] cycloadditions using geometrically flexible tetraenes would be a very significant advance for the synthesis of medicinally important 10-membered ring compounds.[4] Until recently reported discoveries involving dienylfuran systems and electron-deficient alkynes (see examples in Scheme 1), few examples of [8 + 2] cycloadditions employing conformationally flexible systems had been reported.[5,6]

Initial reports of [8 + 2] reactions of *in situ*-generated dienylisobenzofuran intermediates and DMAD (Scheme 1, eq 1) provided a novel method for the synthesis of furanophanes (in some cases, [4 + 2] side products were generated). In subsequent studies, the previously used dienylisobenzofuran intermediates were replaced by stable dienylfurans. Analogous [8 + 2] reactions were observed, resulting in oxygen-bridged 10-membered rings and hydronaphthalene ring systems (Scheme 1, eq 2). The reaction using a *Z*/*E* mixture of dienylfurans with DMAD afforded both the [8 + 2] product and the diene [4 + 2] product. It was suggested that the

Scheme 1. [8 + 2] Reactions Using Furan Systems

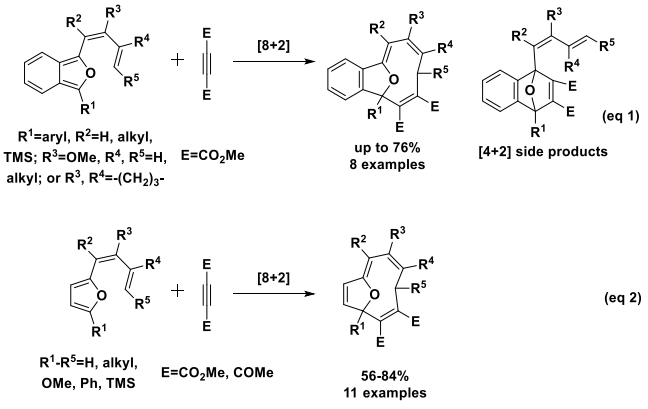

Received: August 12, 2020
Published: January 5, 2021

https://dx.doi.org/10.1021/acs.joc.0c01960
J. Org. Chem. 2021, 86, 1419–1429

reaction of *Z*-dienylfuran and DMAD led to the formation of the [8 + 2] product, while the reaction of *E*-dienylfuran and DMAD led to the formation of the isomerized [4 + 2] product (Scheme 2).[6]

Scheme 2. [8 + 2] and [4 + 2] Reactions Using a *Z*/*E* Mixture of Dienylfuran

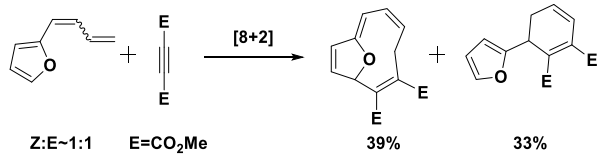

The [8 + 2] reactions could all take place in a concerted superficial−superficial fashion based on the Woodward−Hoffmann rule[7] by counting the number of participating π-electrons in the cycloaddition. This is the proposed pathway A in Scheme 3 for [8 + 2] reactions with the suprafacial orientation. In addition to this pathway, there are several alternative pathways. A stepwise pathway (pathway B) is also possible. This pathway involves initial formation of one C−C bond at the furan terminus of the tetraenes and generation of zwitterionic or diradical intermediates, which then give the cycloadducts after ring closure. Reaction pathway D is similar to reaction pathway B except that the initial C−C bond formation occurs at the other end (C8 atom in Scheme 3) of the diene substituent on furans.

Scheme 3. Proposed Pathways A−E of the [8 + 2] Reactions

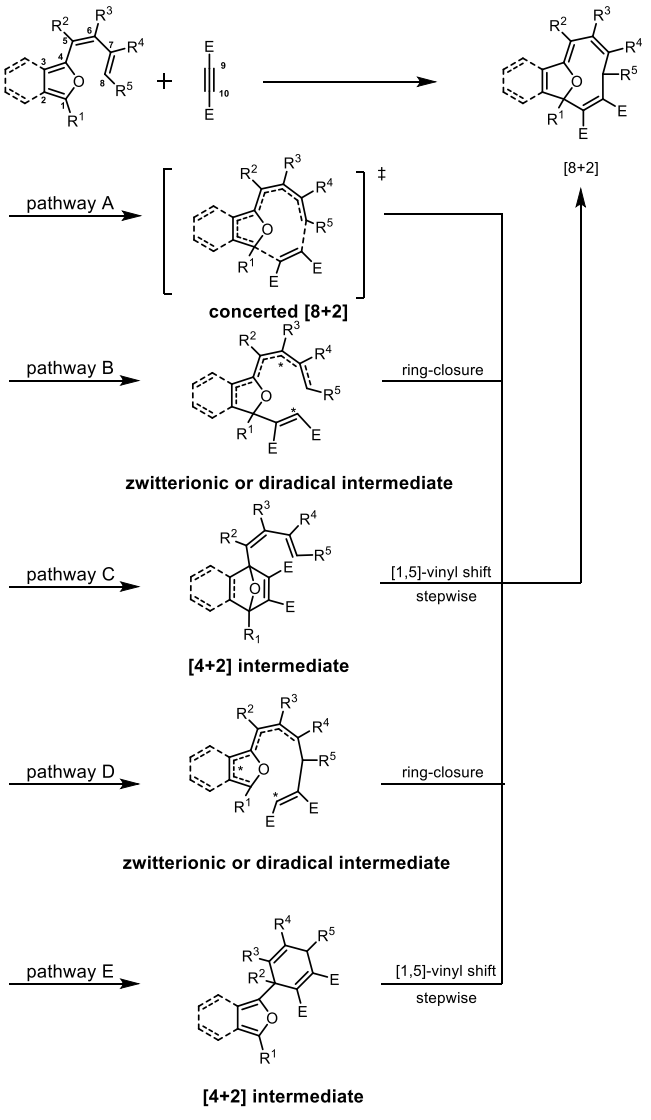

Furans (especially isobenzofurans) undergo [4 + 2] reactions with a variety of different dienophiles.[8] Therefore, we also considered pathway C for the [8 + 2] reaction. This reaction pathway begins with the [4 + 2] reaction of the furan moiety of tetraenes with DMAD followed by the [1,5]-vinyl shift to give the final [8 + 2] cycloadducts. In pathway E, the [8 + 2] reactions begin with an alternative [4 + 2] reactions between the diene part of tetraenes and DMAD followed also by the [1,5]-vinyl shift to give the final cycloadducts.

We previously have studied pathways A−C for the [8 + 2] reaction of dienylisobenzofurans and DMAD.[9] Focus on these pathways was due to the exceptionally high reactivity of the isobenzofuran ring in the substrates. Pathway A can be ruled out because C1 and C8 are far away from each other, and this geometric arrangement makes the concerted [8 + 2] impossible. When there was no electron-donating group present in the diene moieties of dienylisobenzofurans, the [8 + 2] reactions occurred through pathway C. Our previous experimental evidence also supported pathway C. We found that the isolated [4 + 2] cycloadduct undergoes the [1,5]-vinyl shift to give the final [8 + 2] product and the kinetics and activation parameters for this process were determined through NMR measurement of this rearrangement step. When R^3 in dienylisobenzofurans was an electron-donating methoxy group, reaction pathway B to give [8 + 2] products and reaction pathway C to give [4 + 2] products had similar activation energies, leading to formation of both [8 + 2] and [4 + 2] products, respectively. In this case, the [4 + 2] products cannot be converted to [8 + 2] products because the [1,5]-vinyl shift processes were relatively difficult in this case (see later discussion and also the Supporting Information for more details).

Pathways B and C initiate from the isobenzofuran and furan moieties of the tetraenes. Can similar pathways D and E be initiated from the diene part (C5−C6−C7−C8 in Scheme 3) of substrates? We did not consider pathways D and E for the [8 + 2] reaction of dienylisobenzofurans and DMAD since the furan ring of dienylisobenzofurans is far more reactive than its butadiene moiety. But for dienylfurans, these pathways could become more competitive. The furan and linear diene fragments of dienylfurans are both potential reaction sites for Diels−Alder reactions. The evidence for this proposal came from the experimental observation that a diene [4 + 2] product was obtained from the reaction of a *Z*/*E*-dienylfuran mixture with DMAD, in the same reaction pot that also yielded an [8 + 2] product.[6]

The present paper will mainly focus on discussing the reaction mechanisms for the [8 + 2] reaction of simple dienylfurans and DMAD. We discovered that this [8 + 2] reaction prefers pathway D (see the detailed discussion in the Results and Discussion part). We also expanded our study to the [8 + 2] reaction of dienylisobenzofurans with DMAD, to determine whether pathways D and E are possible for these tetraenes. We will also rationalize the diverging reaction pathways for the two systems, which afford structurally similar final [8 + 2] reaction products. Furthermore, we synthesized the pure *Z*-dienylfuran and measured the kinetics of its [8 + 2]

https://dx.doi.org/10.1021/acs.joc.0c01960
J. Org. Chem. 2021, 86, 1419−1429

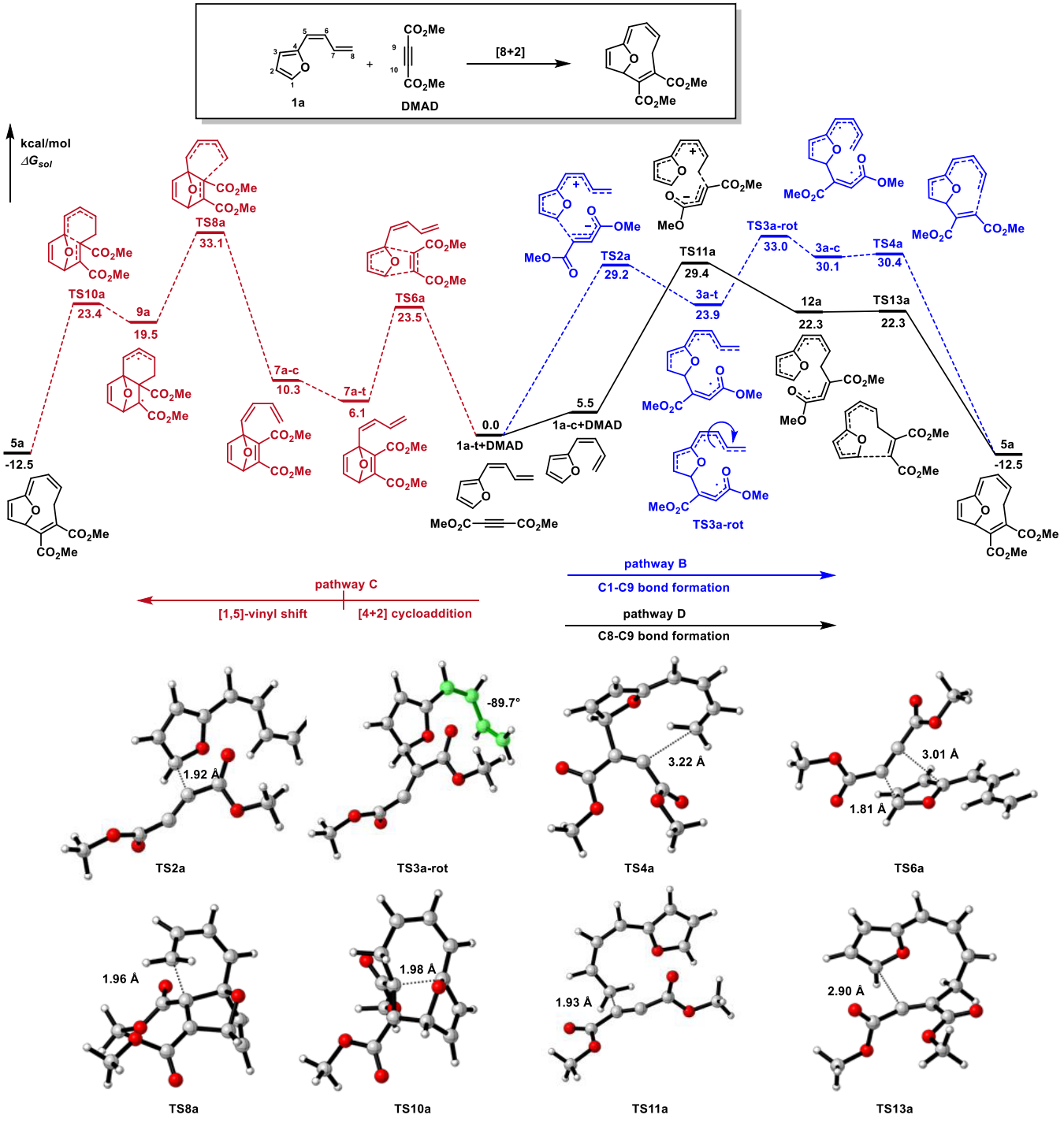

Figure 1. Gibbs energy profiles of pathways B−D of the [8 + 2] reaction between dienylfuran **1** and DMAD computed at the SMD/(U)B3LYP-D3/6-311+G(d,p)//(U)B3LYP/6-31+G(d) level and computed structures of transition states.

cycloaddition with DMAD, aiming to compare the experimental and computational data and to validate the utility of our theoretical methods for this study of the mechanisms of the [8 + 2] reactions.

■ COMPUTATIONAL METHOD

All of the calculations were performed with the Gaussian 09 program.[10] The hybrid B3LYP functional[11] in conjunction with a 6-31+G(d)[12] basis set was applied for the optimization of all stationary points in the gas phase. Diradical intermediates and transition states were located with UB3LYP/6-31+G(d) using keyword: guess = (mix, always). Spin contamination for all singlet diradical stationary points was calculated by the YJH spin contamination correction.[13] Frequency calculations were performed to confirm that each stationary point is either a minimum or a transition structure. Solvent effects in 1,4-dioxane were computed by the SMD model[14] using the gas-phase optimized structures. The computed activation free energies in solution, referred to as ΔG_{sol}, were calculated by adding single point energy in solvation (1,4-dioxane) at (U)B3LYP/6-311+G(d,p) with the D3 version of Grimme's dispersion[15] to the thermal correction to Gibbs free energy at

https://dx.doi.org/10.1021/acs.joc.0c01960
J. Org. Chem. 2021, 86, 1419−1429

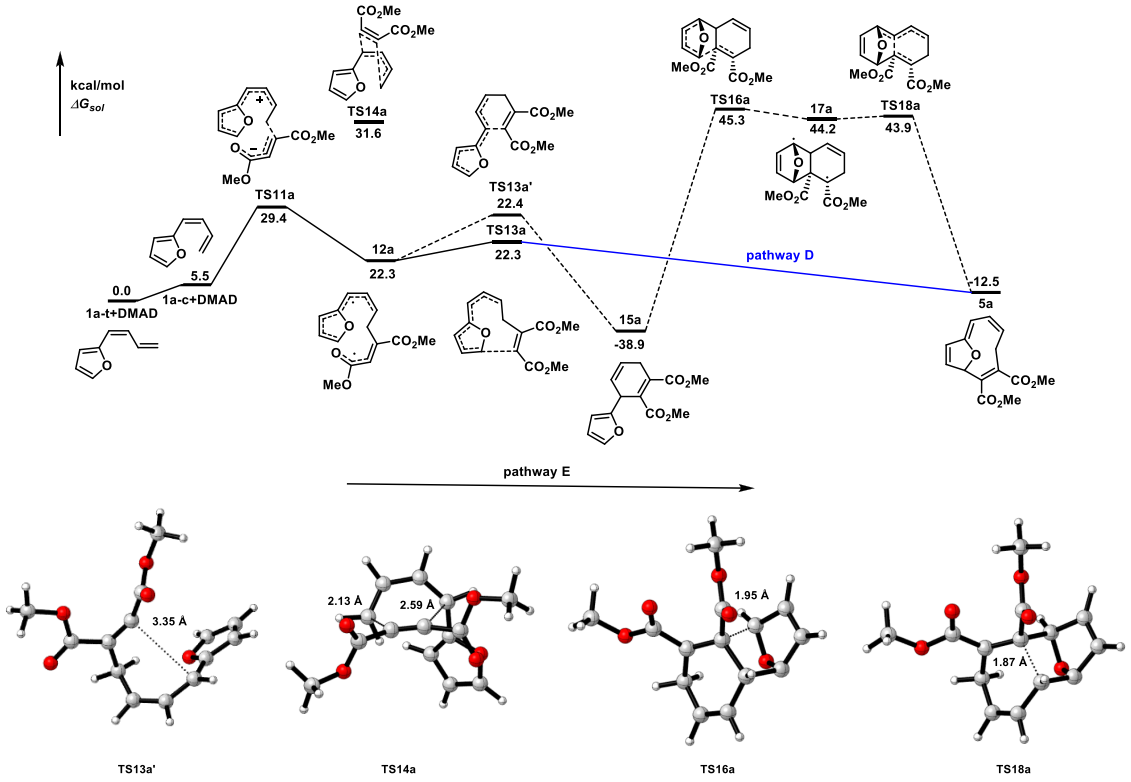

Figure 2. Gibbs energy profiles of pathway E of the [8 + 2] reaction of dienylfuran **1a** with DMAD computed at the SMD/(U)B3LYP-D3/6-311+G(d,p)//(U)B3LYP/6-31+G(d) level and the computed structures of transition states involved in pathway E.

the (U)B3LYP/6-31+G(d) level. Computed structures are illustrated using CYLview.[16] Standard states for solutes in solution are the hypothetical states at 1 M. All discussed energies in the text are Gibbs free energies in solution at 298 K. The molecular orbital energies were computed at the HF/STO-3G level based on the B3LYP/6-31+G(d) geometries in the gas phase. (U)B3LYP has been found to be appropriate to study organic reactions involving diradical intermediates.[17,18] Our kinetic study (see the Results and Discussion part) also show that the computed activation free energy from this functional is close to the experimentally measured value.

RESULTS AND DISCUSSION

Five Possible Pathways of the [8 + 2] Reaction of Dienylfuran and DMAD. We first computed the possible electron transfer from dienylfuran **1a** and DMAD and found that this is energetically impossible (the energy increase is up to 90 kcal/mol), and therefore, this can be excluded for further consideration. Figure 1 shows the DFT-computed energy surfaces of pathways B−D between unsubstituted *Z*-dienylfuran **1a** and DMAD. The DFT-optimized transition states involved in all these pathways are given in Figure 1.

Pathway A. The parent tetraene of dienylfuran **1a** has a stable *s*-trans conformer (**1a-t**). In pathway A, to access the concerted [8 + 2] transition state, **1a** has to convert to its *s*-cis conformer, **1a-c**, so that terminal carbons C1 and C8 are closer to each other (their distances are 4.27 and 5.65 Å for **1a-c** and **1a-t**, respectively). Unfortunately, we failed to locate a concerted [8 + 2] transition state. This failure is well expected, considering the long distance between C1 and C8, which prevents efficient simultaneous orbital overlap of C1 and C8 of dienylfuran with C9 and C10 of DMAD. Therefore, pathway A is not possible and can be excluded from further consideration. This is similar to the [8 + 2] reaction of dienylisobenzofurans and DMAD, which does not have a concerted [8 + 2] transition state either.[9]

Pathway B. The first step of pathway B is the formation of a single C−C bond between C1 of the dienylfuran and C9 of DMAD via a zwitterionic C−C bond forming transition state **TS2a**. In **TS2a**, the C10 atom must point away from the furan ring with the dihedral angle of C10−C9−C1−C4 of 175.4°; otherwise, only concerted [4 + 2] transition structure **TS6a** can be located (see below for the discussion of **TS6a** in pathway C). This C−C bond formation step requires an activation Gibbs free energy of 29.2 kcal/mol. The first step in this pathway leads to the formation of a diradical intermediate **3a-t** with a computed $\langle S^2 \rangle$ of 0.47. The nucleophilic addition of **1** to DMAD to give **3a-t** is endergonic by 23.9 kcal/mol, which can be well understood, considering that this step converts the aromatic furan moiety in the tetraene to a nonaromatic moiety in the intermediate. However, **TS2a** is a closed-shell transition state and its wavefunction is stable, as tested by B3LYP calculations. After that, **3a-t** will transform to its isomer **3a-c** via **TS3a-rot**. This is the rate-determining step of the pathway B with the Gibbs energy barrier of 33.0 kcal/mol related to starting materials **1a** and DMAD. Finally, the product can be formed by a ring-closure transition state via zwitterionic **TS4a**. This step has an activation Gibbs free energy of 0.3 kcal/mol, leading to the formation of cycloadduct **5a**. Therefore, the rate-determining step in pathway B is **TS3a-rot** and the computed Gibbs free activation energy is 33.0 kcal/mol. The [8 + 2] reaction is exergonic by 12.5 kcal/mol.

Pathway C. Pathway C involving the [4 + 2]/[1,5]-vinyl shift is one of the possible pathways in the [8 + 2] reaction of dienylisobenzofuran and DMAD.[9] However, this pathway in the dienylfuran case is not favored at all. Pathway C starts from

https://dx.doi.org/10.1021/acs.joc.0c01960
J. Org. Chem. 2021, 86, 1419−1429

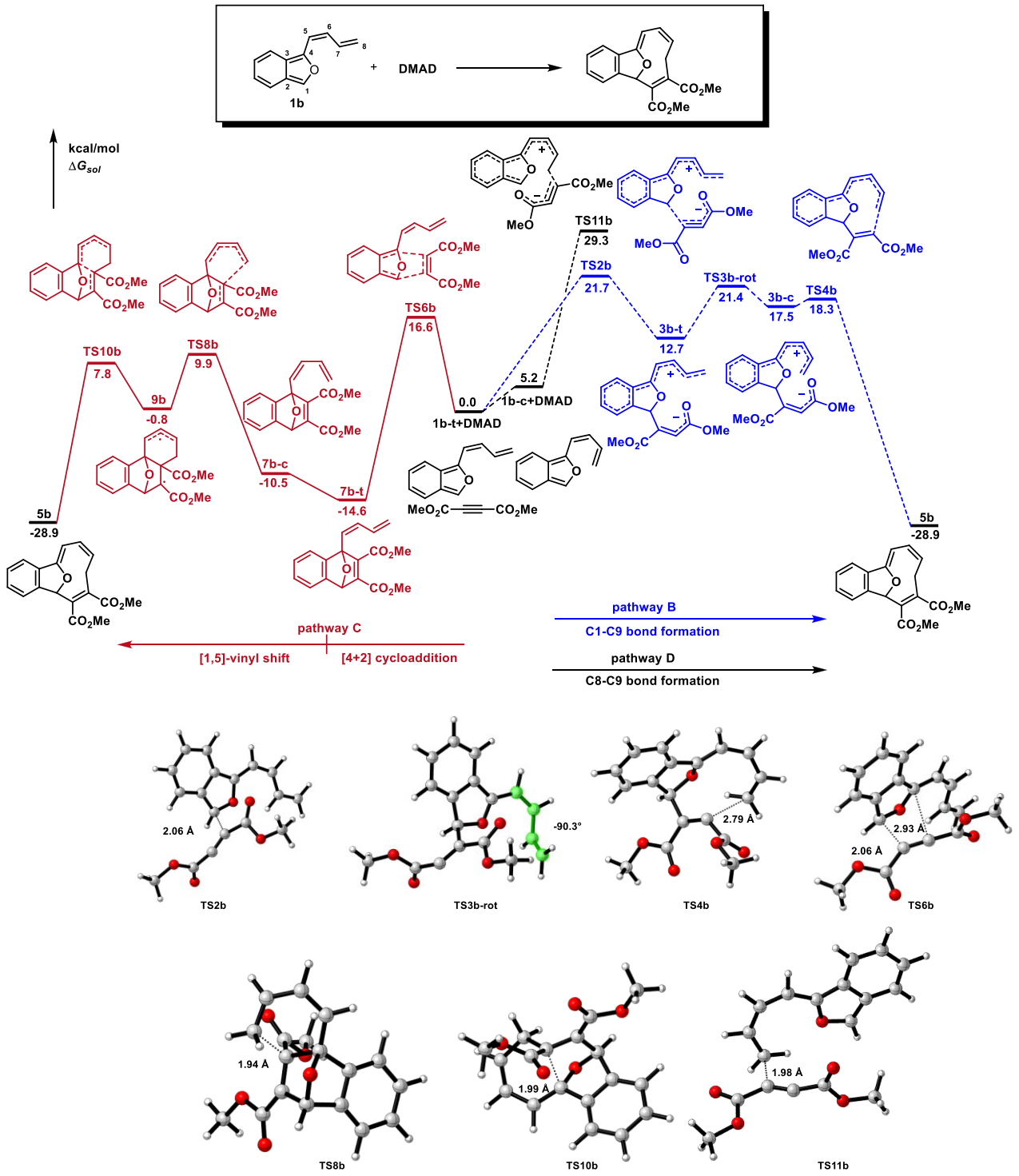

Figure 3. Gibbs energy profiles of pathways B–D of the [8 + 2] reaction between dienylisobenzofuran **1b** and DMAD computed at the SMD/(U)B3LYP-D3/6-311+G(d,p)//(U)B3LYP/6-31+G(d) level and the computed structures of transition states involved in pathways C and D.

a [4 + 2] Diels–Alder cycloaddition between the furan moiety of **1a** and DMAD via transition state **TS6a** with an activation Gibbs free energy of 23.5 kcal/mol. The Diels–Alder reaction is a concerted but asynchronous process. In the [4 + 2] transition state, one forming C–C bond is 1.81 Å while the other C–C bond is 3.01 Å. The following [1,5]-vinyl shift step requires a conformational change. The [4 + 2] cycloadduct **7a-t** undergoes an *s*-trans to *s*-cis interconversion to **7a-c**, which is the reacting conformer for the [1,5]-vinyl shift. This conformational change is usually very easy with less than 10 kcal/mol activation energy.[19] We found that the [1,5]-vinyl shift is stepwise.[20] The first step is forming the C8–C9 bond to give a diradical intermediate **9a** via **TS8a**. Transition state **TS8a** and product **9a** have computed $\langle S^2 \rangle$ values of 0.49 and 1.03, respectively. This step requires an activation Gibbs free energy of 27.0 kcal/mol and is endergonic by 13.4 kcal/mol. The second step of the [1,5]-vinyl shift has the cleavage of the C4–C9 bond from **9a** via **TS10a**. This step is very facile with

https://dx.doi.org/10.1021/acs.joc.0c01960
J. Org. Chem. 2021, 86, 1419–1429

an activation Gibbs free energy of 3.9 kcal/mol and is exergonic by 32.0 kcal/mol. Therefore, if the [8 + 2] reaction occurs in pathway C, the rate-determining step will be the first step of the [1,5]-vinyl shift process with the computed activation Gibbs free energy of 33.1 kcal/mol (via the rate-determining transition state **TS8a**).

Pathway D. The stepwise pathway D proceeds through a similar process as pathway B does. The first step of pathway D is the formation of the C8−C9 bond from **1a-c** via a zwitterionic transition state **TS11a** with an activation Gibbs free energy of 29.4 kcal/mol. In **TS11a**, the newly formed C8−C9 bond distance is 1.93 Å and the C10 of DMAD is far away from the diene moiety in order to reduce the possible steric effects. Formation of the diradical intermediate **12a**, which has a computed $\langle S^2 \rangle$ of 0.93, is endergonic by 22.3 kcal/mol. Ring closure is the second step, which transforms **12a** to the [8 + 2] product **5a** easily via transition state **TS13a**. This second bond-forming **TS13a** is also a singlet diradical transition state. **TS11a** is higher than **TS13a** by 7.1 kcal/mol in terms of Gibbs free energy. Therefore, the rate-determining step of pathway D should be C8−C9 bond formation. The overall activation free energy for pathway D is 29.4 kcal/mol.

Pathway E. Pathway E starts from [4 + 2] cycloaddition of DMAD to the dienyl moiety of dienylfuran followed by the [1,5]-vinyl shift (Figure 2). The concerted [4 + 2] step has an activation free energy of 31.6 kcal/mol via **TS14a**, which is higher than those of pathway D and can be easily ruled out for further consideration. In addition, there is a stepwise [4 + 2] cycloaddition to give **15a**, considering that intermediate **12a** from pathway D can also lead to **15a** by ring closure via **TS13a′**. The computed transition states **TS13a** and **TS13a′** for ring closures to give [8 + 2] and [4 + 2] are close in terms of activation free energy, suggesting that these pathways are possible. However, no [4 + 2] product could be isolated experimentally (see the Experimental Section part in this study).[6] We attributed this discrepancy between experiments and calculations to the inaccuracy of computing singlet diradicals: in the Supporting Information, the relative stabilities of **TS13a** and **TS13a′** depend on the used density functionals for calculations. Therefore, we proposed that pathway E takes place via a stepwise [4 + 2] to give **15a**, but this is not favored compared to pathway D.

In addition, we can further exclude pathway E by considering the thermodynamic of its [4 + 2] step. We found that the [4 + 2] step leads to the formation of an intermediate **15a**, which is much more stable than the [8 + 2] cycloadduct **5a**. Kinetically, this transformation is not possible. The possible [1,5]-vinyl shift via structurally twisted diradical species **TS16a**, **17a**, and **TS18a** to give the [8 + 2] cycloadduct is stepwise, with the activation Gibbs energy of more than 80 kcal/mol. The high energy here is due to disrupting the aromaticity of furan and the distorted bond in **TS16a**. Therefore, this pathway can be excluded directly.

Comparison of Pathways A−E. By comparing the computed energy surfaces of pathways B−E, which need activation Gibbs free energies of 33.0, 33.1, 29.4, and 84.2 kcal/mol, respectively, we can conclude that pathway D is the most favored one. The computational results indicate that if an [8 + 2] cycloadduct is obtained, the reaction would take place through pathway D. No reaction intermediate could be isolated since the intermediate in this pathway is higher in energy than the reactants by 22.3 kcal/mol in terms of Gibbs free energy. The preference of pathway D for *Z*-dienylfuran over pathway C is completely different from dienylisobenzofurans, which prefer to react with DMAD via pathway C instead of pathway D. These calculation results can explain why no [4 + 2] product **7a-t** was observed in the reactions of pure *Z*-dienylfurans with DMAD (see Figure 1).

[8 + 2] Reaction of Dienylisobenzofurans with DMAD. As mentioned above, we only considered pathways A−C in a previous study on the mechanism of [8 + 2] reactions of dienylisobenzofurans with DMAD.[9] Pathways D and E were not considered; however, pathway E can be easily ruled out based on the above study. Here, we reconsider the possibility of the pathway D and the comparison of these competing pathways (Figure 3). Similarly, the electron-transfer mechanisms for dienylisobenzofurans and DMAD are disfavored in the present case (endogenic by about 80 kcal/mol).

Pathway B is a stepwise [8 + 2] reaction via **TS2b**, **3b-t**, **TS3b-rot**, **3b-c**, and **TS4b**. The first step is the rate-determining step to give the zwitterionic intermediate **3b-t**. After transforming to **3b-c** via **TS3b-rot**, the reaction easily undergoes the ring closure to give the [8 + 2] cycloadduct instead of transforming back to the reactants. Therefore, the activation free energy for this pathway is 21.7 kcal/mol. For pathway C, the first step is an irreversible [4 + 2] cycloaddition with a computed activation free energy of 16.6 kcal/mol. The following [1,5]-vinyl shift from **7b-t** to the [8 + 2] product is also stepwise via **TS8b**, **9b**, and **TS10b**. Previously, we missed the first step of the stepwise [1,5]-vinyl shift. Therefore, our previous calculations underestimated the barrier of the [1,5]-vinyl shift by a few kcal/mol because the first step is more difficult than the second step in the [1,5]-vinyl shift. Fortunately, this does not affect our previous conclusions of the mechanism of the [8 + 2] reaction of dienylisobenzofurans with DMAD because the [4 + 2] step in this pathway is irreversible. For pathway D, we found that the first step is the formation of the C8−C9 bond via a zwitterionic transition structure **TS11b** with an activation free energy of 29.3 kcal/mol, which is a difficult process compared to processes B and C (via **TS2b** and **TS6b**, respectively), so pathway D is disfavored and should be ruled out.

From the comparison of the Gibbs energy profile of pathways B−D, we found that the most favorable pathway is pathway C, which is in agreement of our previous work. From pathway C, we can find that the [4 + 2] step is irreversible and the rate-determining step is the [1,5]-vinyl shift. The overall activation free energy for this [8 + 2] reaction is 24.5 kcal/mol (from **7b-t** to **TS8b**).

We have also studied other [8 + 2] reactions of dienylisobenzofurans with DMAD for all pathways and found that our previous mechanisms still hold and pathway D is not competitive except for those substrates having an electron-donating alkoxyl group at the C6 position (see later on DFT Study of Two More [8 + 2] Reactions of Dienylisobenzofurans with DMAD in Real Model of the present study and the Supporting Information).

FMO Analysis to Explain Why Two [8 + 2] Reactions Have Different Pathways. To explain the preference for pathway D with dienylfurans and the preference for pathway C with dienylisobenzofurans, we performed an FMO analysis (Figure 4).

In dienylisobenzofuran, the HOMO orbital coefficients of C1 and C4 are close but both are larger than C8, suggesting that C8 is less nucleophilic in cycloaddition compared to both

https://dx.doi.org/10.1021/acs.joc.0c01960
J. Org. Chem. 2021, 86, 1419−1429

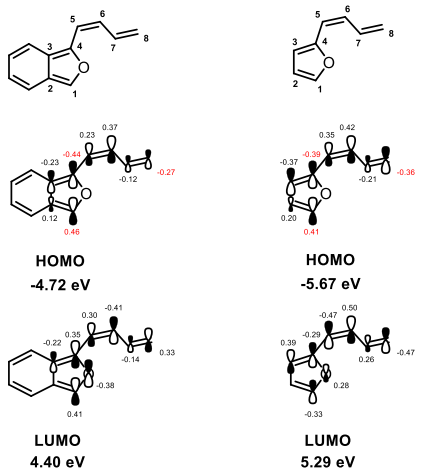

Figure 4. Frontier molecular orbitals and energies of dienylisobenzofuran and dienylfuran computed by the HF/STO-3G method based on the gas-phase B3LYP/6-31+G(d) geometries. The orbital coefficients refer to the 2p part of each heavy atom.

C1 and C4. Therefore, dienylisobenzofuran prefers to react with alkyne through the pathway C ([4 + 2]/[1,5]-vinyl shift) than pathway D. Also, formation of a more aromatic benzene ring in isobenzofuran systems can also promote the [4 + 2]/[1,5]-vinyl shift pathway C. In the dienylfuran case, the HOMO orbital coefficients of C1, C4, and C8 are very close to each other. This means that C1 and C8 have the same tendency to act as nucleophiles. Meanwhile, when considering the aromaticity of the intermediate **7a-t** in pathway C of Figure 1, obviously, the aromatic ring is destroyed for **7a-t** (aromatic benzene ring is forming for dienylisobenzofurans). Therefore, pathways B and D could be more competitive. Considering that the transformation from **3a-t** to **3a-c** is not easy, the pathway D is more favorable in this case.

DFT Study of Two More [8 + 2] Reactions of Dienylisobenzofurans with DMAD in Real Model. We also studied the mechanisms of the [8 + 2] reactions of substituted dienylisobenzofurans with DMAD, which had been previously investigated both experimentally and computationally by us.[9] In previous DFT studies, we did not include a Ph group in the benzofuran part of these dienylisobenzofurans and the previous conclusions of mechanisms could be revised when the exact tetraenes were used in calculations (Figure 5).

In the case of **1c-t** and DMAD, pathways B and D are not favorable, with the activation Gibbs energies of 26.1 and 24.8 kcal/mol, respectively. Pathway C is favorable with a relatively easy [4 + 2] cycloaddition via **TS6c** to give the intermediate **7c-t**. Then, like the similar process discussed before, **7c-c** goes a stepwise [1,5]-vinyl shift (through **TS8c**, **9c**, and **TS10c**) to give the final [8 + 2] cycloadduct **5c**. The activation Gibbs energy of the [1,5]-vinyl shift from **7c-t** is 24.8 kcal/mol. We previously synthesized **7c-t** and measured the kinetic data of the reaction from **7c-t** to **5c**, finding that an activation Gibbs energy of 24.2 kcal/mol is required for this transformation.[9] This consistency between experimental and computational values indicates that our calculation methods are reliable in evaluating the present [8 + 2] reactions.

For the case of dienylisobenzofuran with an electron-donating OMe group at the C6 position, a full model of the reaction with **1d** and DMAD was studied. Previously, we proposed that both pathways B and C compete with each other to give [4 + 2] and [8 + 2] products, respectively. We found previously that the [8 + 2] product **5d** and [4 + 2] product **7d** can be isolated when heating the mixture of **1d** and DMAD. However, for the [1,5]-vinyl shift in pathway C, the compound **7d** decomposed upon further heating. We did not consider pathway D at that time. Here, we tried to rationalize this reaction by considering pathway D, which could be favored over pathway B because the diene part has an electron-donating MeO group to promote its reaction with DMAD.

The activation Gibbs free energies of the first step in pathways B−D via the transition states **TS2d**, **TS6d**, and **TS11d** are 28.3, 22.3, and 24.4 kcal/mol, respectively. So, the pathway B is disfavored here. Therefore, both [4 + 2] (from pathway C) and [8 + 2] (via pathway D) products would be formed, which is consistent with experimental results.

The [4 + 2] product was predicted to undergo the [1,5]-vinyl shift easily with a computed activation free energy of 19.2 kcal/mol. However, experimentally heating this cycloadduct afforded decomposition products.[9] Here, we give an explanation for this discrepancy between experiments and DFT calculations. The present DFT-computed activation free energy of the [1,5]-vinyl shift is close to the experimental result for **7c-t** (see above), suggesting that the computed activation free energy of the [1,5]-vinyl shift for **7d** here could be reasonable too. However, the activation free energies for **TS6d** and **TS11d** could be overestimated due to entropy overestimation for bimolecular reactions.[21] This means that these two processes via pathways C and D could have activation free energies lower than 19.2 kcal/mol, which is required for the [1,5]-shift in this reaction. But in the reaction, both [4 + 2] and [8 + 2] products can be obtained kinetically at lower temperature. Consequently, the [1,5]-vinyl shift for **7d** needs higher barrier and higher temperature, compared to the [4 + 2] reaction step in pathway C and the direct [8 + 2] reaction via pathway D. Unfortunately, heating **7d** at higher temperature leads to decomposed products due to unknown but easier side reactions, compared to the [1,5]-vinyl shift reaction.

Kinetic Study. In order to determine whether our calculation methods used here are reliable or not for the present system, we measured the kinetic data of the [8 + 2] reaction of dienylfuran and DMAD. First, (*Z*)-2-(buta-1,3-dien-1-yl)furan **1a** was synthesized by the route shown in Scheme 4.[22] Using furfural as the starting material, the intermediate allylsilane-alcohol was obtained as an erythro-diastereomer via titanium(IV)-mediated nucleophilic addition of an allyltrimethylsilane anion at −78 °C. Without further purification, the silyl alcohol was transformed to the *Z*-dienylfuran by treatment with potassium hydride at low temperature. This Peterson olefination sequence led to the formation of *Z*-dienylfuran with a *Z*/*E* ratio of greater than 20:1.

Then, we measured the kinetic data by monitoring *in situ* the NMR spectrum of the [8 + 2] reaction of *Z*-dienylfuran **1a** (1 equiv) with DMAD (10 equiv) at 70, 75, 80, and 85 °C (see Figure 6 and the Supporting Information for details). The kinetic data can provide the observed rate constant, $k_{obs} = 3.08 \times 10^7 \exp(-18.8/RT)$ (s^{-1}), and the activation energy, E_a = 18.0 kcal/mol. Based on the Eyring plot, the measured $\Delta H^{\ddagger}$, $\Delta S^{\ddagger}$, and $\Delta G^{\ddagger}$ values are 18.1 kcal/mol, −26.6 cal/(mol K), and 26.0 kcal/mol, respectively. The DFT-computed $\Delta G^{\ddagger}$ value is 29.4 kcal/mol in 1,4-dioxane, which is 3.4 kcal/mol higher than the experimental value. Considering the overestimation of entropy in bimolecular reactions,[21] we can see

https://dx.doi.org/10.1021/acs.joc.0c01960
J. Org. Chem. 2021, 86, 1419−1429

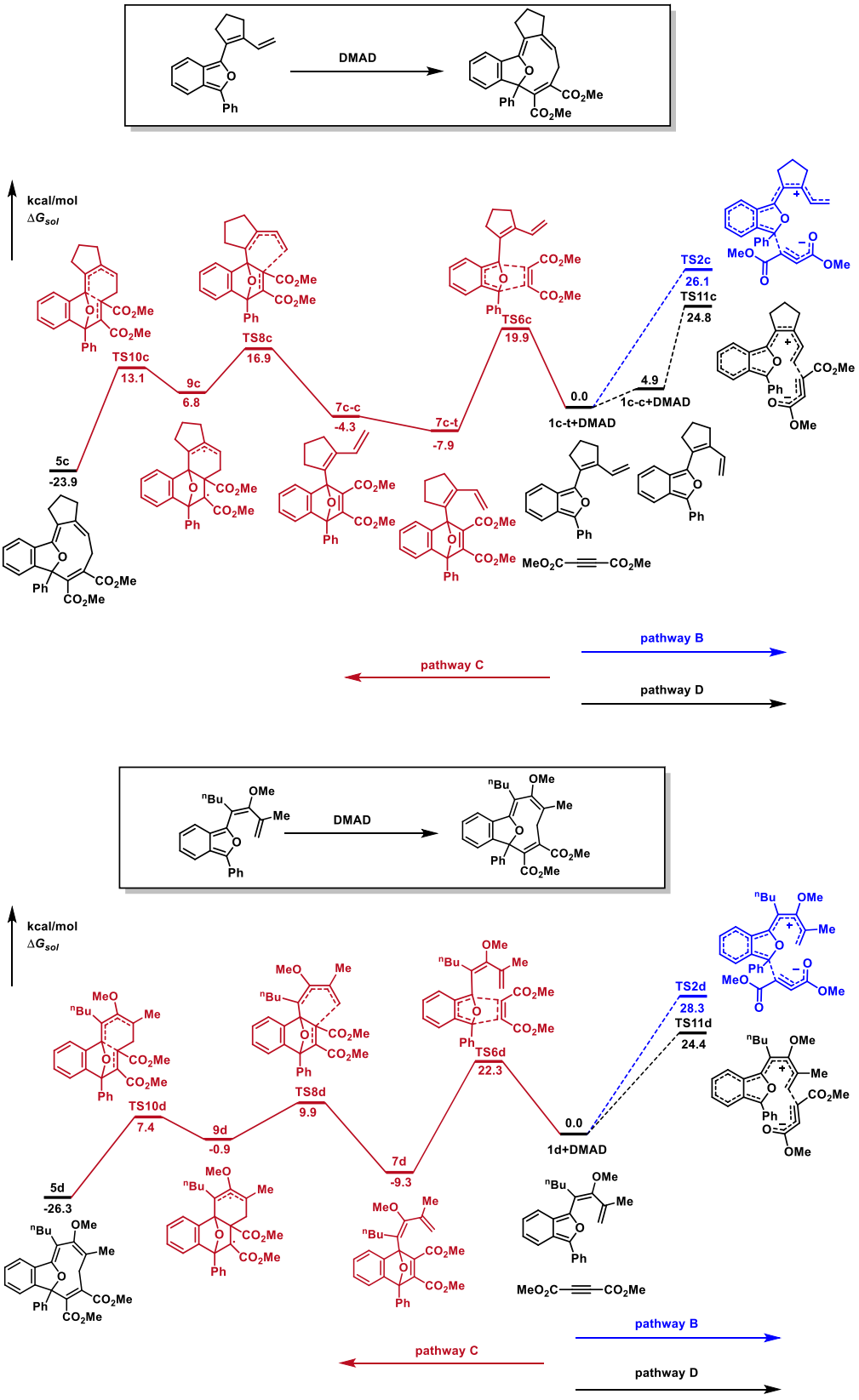

Figure 5. Gibbs energy profiles of pathways B–D of the [8 + 2] reaction between substituted dienylisobenzofurans **1c** and **1d** and DMAD computed at the SMD/(U)B3LYP-D3/6-311+G(d,p)//(U)B3LYP/6-31+G(d) level.

that the results from DFT computations and experiments are in accordance, suggesting that the present computational method is reliable for study of this pericyclic reaction.

https://dx.doi.org/10.1021/acs.joc.0c01960
J. Org. Chem. 2021, 86, 1419–1429

Scheme 4. Synthesis of (*Z*)-2-(Buta-1,3-dien-1-yl)furan 1a and [8 + 2] Reaction of 1a with DMAD

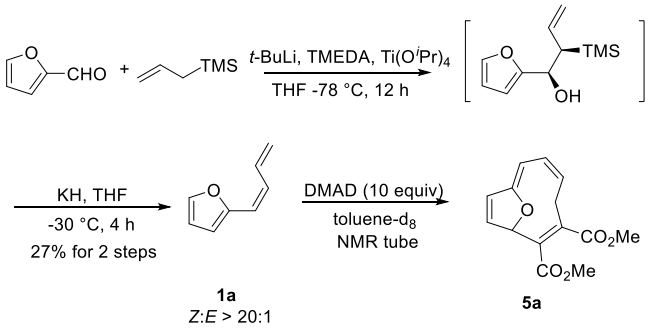

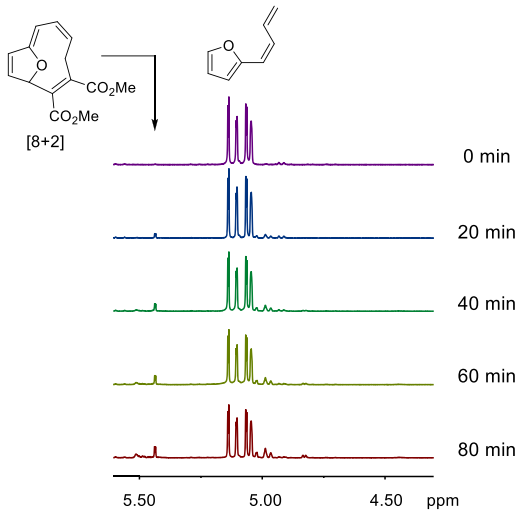

Figure 6. Monitoring of the changes of the ^{1}H NMR spectrum over time for the [8 + 2] reaction of (*Z*)-2-(buta-1,3-dien-1-yl)furan **1a** and DMAD in toluene-d_8 at 70 °C.

CONCLUSIONS

In conclusion, we have used DFT calculations to study the mechanisms of [8 + 2] reactions of dienylfurans/dienylisobenzofurans and DMAD (Scheme 5). For dienylfurans, the [8 + 2] reaction prefers a new course, pathway D, starting from attack of the acyclic diene moiety, not the furyl moiety in dienylfurans, to DMAD to give a diradical intermediate, which then undergoes ring closure to form the second bond between DMAD and the furan moiety. For dienylisobenzofurans, the [8 + 2] reaction favors pathway C, beginning from [4 + 2] cycloaddition of the diene in the furan ring of dienylisobenzofurans toward DMAD followed by the rate-determining stepwise [1,5]-vinyl shift. The different mechanisms of [8 + 2] reactions have been analyzed, finding that for dienylfurans, their reactive diene part is the diene substituent, not the furan moiety; but for dienylisobenzofurans, their reactive diene part is the diene in the furan ring. Also, FMO theory has been used to analyze the different reaction sites and pathways. The substituent effects for the [8 + 2] reaction of dienylisobenzofurans with DMAD have also been reinvestigated by DFT calculations, showing that pathways B and C compete (while pathway D could also happen when the diene substituent on furan has an electron-donating group and R^1 = phenyl).

Scheme 5. Summary of the [8 + 2] Reactions in Different Pathways

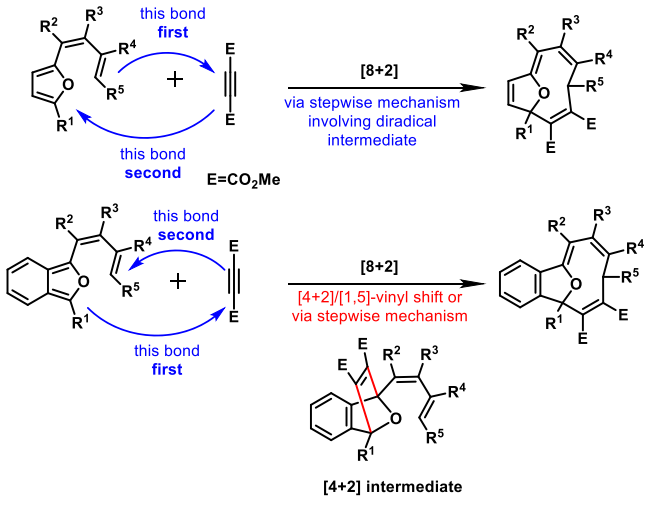

EXPERIMENTAL SECTION

Preparation of (*Z*)-2-(Buta-1,3-dien-1-yl)furan 1a (Scheme 4). In an oven-dried 200 mL round-bottom flask, allyltrimethylsilane (5.6 g, 49 mmol) was added, followed by the addition of THF (50 mL) and tetramethylethylenediamine (TMEDA) (6.8 mL, 44 mmol) under an argon atmosphere. To this solution was added *t*-butyllithium (34.0 mL of a 1.3 M pentane solution, 44 mmol) slowly at −78 °C. The reaction mixture was allowed to warm to −30 °C over a 1 h period and stirred at −30 °C for another 1 h. The reaction mixture was cooled to −78 °C, and then Ti(O^{i}Pr)$_4$ (14.0 mL, 49 mmol) was added (the color became red). After 1 h, furfural (3.3 mL, 40 mmol) was added dropwise at −78 °C and the reaction mixture was stirred at −78 °C for 12 h. The reaction mixture was then quenched at −78 °C by the addition of aqueous ammonium chloride solution followed by warming to room temperature and adding saturated aqueous potassium sodium tartrate tetrahydrate solution at room temperature. The mixture was extracted with ether, and the ether layer was washed with brine and dried over sodium sulfate. The organic solvent was removed on a rotary evaporator, and the residue after evaporation was a reddish oil. The crude product was used in the next step without further purification.

In a 250 mL flask under argon, potassium hydride (10.25 g, 30% in mineral oil, 77 mmol) was added and washed three times with pentane (20 mL). After pumping out the residual pentane, the solvent THF (70 mL) was added. The reaction mixture was cooled to −78 °C, and a solution of the crude product from the first step in THF (30 mL) was added very carefully. The mixture was allowed to warm to −35 °C and stirred for 4 h. The reaction was monitored by TLC analysis until the reactant was fully consumed. The reaction was quenched by very careful addition of water. The mixture was extracted with pentane (3 × 200 mL), and the combined organic layers were washed with water (2 × 250 mL) and brine (250 mL). After drying over sodium sulfate, the mixture was filtered and the solvent was removed very carefully at 0 °C, 200 to 50 mbar on a rotary evaporator. The product was purified by distillation (70−72 °C, 40 mbar). A colorless oil identified as *Z*-dienylfuran **1a** (1.31 g, 27% yield over two steps, *Z*/*E* > 20:1) was obtained after final purification. The NMR spectra were consistent with the reported literature.[23] TLC R_f = 0.67 (PE). ^{1}H NMR ($CDCl_3$, 400 MHz): δ 7.44 (d, J = 1.8 Hz, 1H), 7.37 (ddd, J = 16.9, 10.3, 10.0 Hz, 1H), 6.41 (dd, J = 3.3, 1.8 Hz, 1H), 6.33 (d, J = 3.3 Hz, 1H), 6.09 (dd, J = 11.8, 10.0 Hz, 1H), 6.08 (d, J = 11.8 Hz, 1H), 5.36 (dd, J = 16.9, 1.9 Hz, 1H), 5.27 (dd, J = 10.3, 1.9 Hz, 1H). ^{13}C{H} NMR ($CDCl_3$, 101 MHz): δ 153.6, 142.5, 134.4, 127.8, 119.9, 117.1, 111.4, 110.8. HRMS (EI) *m*/*z*: [M·]$^+$ calcd for C_8H_8O, 120.0570; found, 120.0572.

Kinetic Study of [8 + 2] Reaction of (*Z*)-2-(Buta-1,3-dien-1-yl)furan 1a and DMAD. In a 10.00 mL volumetric flask, *Z*-dienylfuran **1a** (120.1 mg, 1.0 mmol), DMAD (1.43 g, 10 equiv), and an internal standard (*n*-$C_{12}H_{26}$, 16.9 mg, 0.1 equiv) were added,

https://dx.doi.org/10.1021/acs.joc.0c01960
J. Org. Chem. 2021, 86, 1419−1429

followed by toluene-d_8 sufficient to achieve a total volume of 10.00 mL. Each of NMR tubes was added 500 μL of this solution using a syringe. These NMR tubes were heated separately at 70, 75, 80, and 85 °C for different times (see the Supporting Information for details). After the designated time, they were placed into an ice water bath and examined by 500 MHz ^{1}H NMR for 32 scans. The ratio of *Z*-dienylfuran and internal standard was determined by the integrals at δ = 5.030−5.150 and δ = 0.760−0.835, respectively.

Checking the Possible [4 + 2] Product of [8 + 2] Reaction of (*Z*)-2-(Buta-1,3-dien-1-yl)furan 1a and DMAD. We checked the crude NMR of the reaction and did not see the presence of the [4 + 2] product. Therefore, we can rule out pathway E via **TS13a′** in Figure 2.

■ ASSOCIATED CONTENT

Supporting Information

The Supporting Information is available free of charge at https://pubs.acs.org/doi/10.1021/acs.joc.0c01960.

Computed enthalpies and Gibbs free energies in the gas phase, potential energy surfaces of the reaction of dienylisobenzoburans and dienophiles, other reaction pathways and discussion of calculation methods, experimental part (NMR spectra of **1a** and kinetic studies), computed energies of all of the stationary points, and Cartesian coordinates of all computed structures (PDF)

■ AUTHOR INFORMATION

Corresponding Author

Zhi-Xiang Yu − *Beijing National Laboratory for Molecular Sciences (BNLMS), Key Laboratory of Bioorganic Chemistry and Molecular Engineering of the Ministry of Education, College of Chemistry, Peking University, Beijing 100871, P. R. China*; orcid.org/0000-0003-0939-9727; Email: yuzx@pku.edu.cn

Authors

Qi Cui − *Beijing National Laboratory for Molecular Sciences (BNLMS), Key Laboratory of Bioorganic Chemistry and Molecular Engineering of the Ministry of Education, College of Chemistry, Peking University, Beijing 100871, P. R. China*

Yuanyuan Chen − *Beijing National Laboratory for Molecular Sciences (BNLMS), Key Laboratory of Bioorganic Chemistry and Molecular Engineering of the Ministry of Education, College of Chemistry, Peking University, Beijing 100871, P. R. China*

James W. Herndon − *Department of Chemistry and Biochemistry, New Mexico State University, Las Cruces, New Mexico 88003, United States*

Complete contact information is available at: https://pubs.acs.org/10.1021/acs.joc.0c01960

Notes

The authors declare no competing financial interest.

■ ACKNOWLEDGMENTS

This work was supported by the National Natural Science Foundation of China (21933003) and High-Performance Computing Platform of Peking University.

■ REFERENCES

(1) von E. Doering, W.; Wiley, D. W. Heptafulvene-(methylenecycloheptatriene). *Tetrahedron* **1960**, *11*, 183−198.

(2) For reviews of [8+2] and other high-order cycloadditions, see: (a) Frankowski, S.; Romaniszyn, M.; Skrzyńska, A.; Albrecht, Ł. The Game of Electrons: Organocatalytic Higher-Order Cycloadditions Involving Fulvene- and Tropone-Derived Systems. *Chem. − Eur. J.* **2020**, *26*, 2120−2132. (b) McLeod, D.; Thøgersen, M. K.; Jessen, N. I.; Jørgensen, K. A.; Jamieson, C. S.; Xue, X.-S.; Houk, K. N.; Liu, F.; Hoffmann, R. Expanding the Frontiers of Higher-Order Cycloadditions. *Acc. Chem. Res.* **2019**, *52*, 3488−3501. (c) Nair, V.; Abhilash, K. [8+ 2] Cycloaddition reactions in organic synthesis. *Synlett* **2008**, 301−312.

(3) For selected recent examples: (a) Mose, R.; Preegel, G.; Larsen, J.; Jakobsen, S.; Iversen, E. H.; Jørgensen, K. A. Organocatalytic stereoselective [8+2] and [6+4] cycloadditions. *Nat. Chem.* **2017**, *9*, 487−492. (b) Xie, M.; Liu, X.; Wu, X.; Cai, Y.; Lin, L.; Feng, X. Catalytic Asymmetric [8+2] Cycloaddition: Synthesis of Cycloheptatriene-Fused Pyrrole Derivatives. *Angew. Chem., Int. Ed.* **2013**, *52*, 5604−5607. (c) Xie, M.; Wu, X.; Wang, G.; Lin, L.; Feng, X. Catalytic Asymmetric [8+2] Cycloaddition for the Construction of Cycloheptatriene-Fused Pyrrolidin-3,3'-Oxindoles. *Acta Chim. Sin.* **2014**, *72*, 856−861.

(4) (a) Ellis, J. M.; Crimmins, M. T. Strategies for the Total Synthesis of C2− C11 Cyclized Cembranoids. *Chem. Rev.* **2008**, *108*, 5278−5298. (b) Welford, A. J.; Collins, I. The 2, 11-cyclized cembranoids: Cladiellins, asbestinins, and briarellins (period 1998−2010). *J. Nat. Prod.* **2011**, *74*, 2318−2328.

(5) Luo, Y.; Herndon, J. W.; Cervantes-Lee, F. Synthesis of furanophane derivatives through [8+2]-cycloaddition of dienylisobenzofurans and alkynes. *J. Am. Chem. Soc.* **2003**, *125*, 12720−12721.

(6) (a) Zhang, L.; Wang, Y.; Buckingham, C.; Herndon, J. W. Synthesis of furan-bridged 10-membered rings through [8+2]-cycloaddition of dienylfurans and acetylenic esters. *Org. Lett.* **2005**, *7*, 1665−1667. (b) Ying, W.; Zhang, L.; Wiget, P. A.; Herndon, J. W. A novel stereoselective [8+2] double cycloaddition route to hydronaphthalene ring systems. *Tetrahedron Lett.* **2016**, *57*, 2954−2956.

(7) (a) Hoffmann, R.; Woodward, R. B. Selection Rules for Concerted Cycloaddition Reactions. *J. Am. Chem. Soc.* **1965**, *87*, 2046−2048. (b) Hoffmann, R.; Woodward, R. B. Conservation of orbital symmetry. *Acc. Chem. Res.* **1968**, *1*, 17−22. (c) Woodward, R. B.; Hoffmann, R. The conservation of orbital symmetry. *Angew. Chem., Int. Ed. Engl.* **1969**, *8*, 781−853.

(8) For a review of furan Diels−Alder reactions, see: (a) Kappe, C. O.; Murphree, S. S.; Padwa, A. Synthetic applications of furan Diels-Alder chemistry. *Tetrahedron* **1997**, *53*, 14179−14233. (b) For a review of isobenzofurans, see: Friedrichsen, W. Recent advances in the chemistry of benzo [c] furans and related compounds. *Adv. Heterocycl. Chem.* **1999**, *73*, 1−96.

(9) Chen, Y.; Ye, S.; Jiao, L.; Liang, Y.; Sinha-Mahapatra, D. K.; Herndon, J. W.; Yu, Z.-X. Mechanistic Twist of the [8+2] Cycloadditions of Dienylisobenzofurans and Dimethyl Acetylenedicarboxylate: Stepwise [8+2] versus [4+2]/[1,5]-Vinyl Shift Mechanisms Revealed through a Theoretical and Experimental Study. *J. Am. Chem. Soc.* **2007**, *129*, 10773−10784.

(10) *Gaussian 09, Revision E.01*, Frisch, M. J.; Trucks, G. W.; Schlegel, H. B.; Scuseria, G. E.; Robb, M. A.; Cheeseman, J. R.; Scalmani, G.; Barone, V.; Mennucci, B.; Petersson, G. A.; Nakatsuji, H.; Caricato, M.; Li, X.; Hratchian, H. P.; Izmaylov, A. F.; Bloino, J.; Zheng, G.; Sonnenberg, J. L.; Hada, M.; Ehara, M.; Toyota, M.; Fukuda, R.; Hasegawa, J.; Ishida, M.; Nakajima, T.; Honda, Y.; Kitao, O.; Nakai, H.; Vreven, T.; Montgomery, J. A., Jr.; Peralta, J. E.; Ogliaro, F.; Bearpark, M.; Heyd, J. J.; Brothers, E.; Kudin, K. N.; Staroverov, V. N.; Keith, T.; Kobayashi, R.; Normand, J.; Raghavachari, K.; Rendell, A.; Burant, J. C.; Iyengar, S. S.; Tomasi, J.; Cossi, M.; Rega, N.; Millam, J. M.; Klene, M.; Knox, J. E.; Cross, J. B.; Bakken, V.; Adamo, C.; Jaramillo, J.; Gomperts, R.; Stratmann, R. E.; Yazyev, O.; Austin, A. J.; Cammi, R.; Pomelli, C.; Ochterski, J. W.; Martin, R. L.; Morokuma, K.; Zakrzewski, V. G.; Voth, G. A.; Salvador, P.; Dannenberg, J. J.; Dapprich, S.; Daniels, A. D.; Farkas,

O.; Foresman, J. B.; Ortiz, J. V.; Cioslowski, J.; Fox, D. J. Gaussian, Inc.: Wallingford CT, 2013.
(11) (a) Becke, A. D. Density-functional thermochemistry. III. The role of exact exchange. *J. Chem. Phys.* **1993**, *98*, 5648−5652. (b) Lee, C.; Yang, W.; Parr, R. G. Development of the Colle-Salvetti correlation-energy formula into a functional of the electron density. *Phys. Rev. B* **1988**, *37*, 785−789.
(12) Hehre, W. J., Radom, L., Schleyer, P. v. R.; Pople, J. A. *Ab Initio Molecular Orbital Theory;* Wiley: New York, 1986.
(13) Yamaguchi, K.; Jensen, F.; Dorigo, A.; Houk, K. N. *Chem. Phys. Lett.* **1988**, *149*, 537−542.
(14) Marenich, A. V.; Cramer, C. J.; Truhlar, D. G. Universal solvation model based on solute electron density and on a continuum model of the solvent defined by the bulk dielectric constant and atomic surface tensions. *J. Phys. Chem. B* **2009**, *113*, 6378−6396.
(15) Grimme, S.; Antony, J.; Ehrlich, S.; Krieg, H. A consistent and accurate ab initio parametrization of density functional dispersion correction (DFT-D) for the 94 elements H-Pu. *J. Chem. Phys.* **2010**, *132*, 154104.
(16) Legault, C. Y. CYLview, 1.0b, Universitéde Sherbrooke, 2009. http://www.cylview.org.
(17) (a) Zhai, L.; Tian, X.; Wang, C.; Cui, Q.; Li, W.; Huang, S. H.; Yu, Z.-X.; Hong, R. Construction of Morphan Derivatives by Nitroso-Ene Cyclization: Mechanistic Insight and Total Synthesis of (±)-Kopsone. *Angew. Chem., Int. Ed.* **2017**, *56*, 11599−11603. (b) James, N. C.; Um, J. M.; Padias, A. B.; Hall, H. K., Jr.; Houk, K. N. Computational Investigation of the Competition between the Concerted Diels−Alder Reaction and Formation of Diradicals in Reactions of Acrylonitrile with Nonpolar Dienes. *J. Org. Chem.* **2013**, *78*, 6582−6592. (c) Cai, P.-J.; Shi, F.-Q.; Wang, Y.; Li, X.; Yu, Z.-X. Homopyrrole and Homofuran as Masked 1, 5-Dipoles in Metal-Free (5+2) Cycloadditions with Dienophiles: A DFT Study. *Tetrahedron* **2013**, *69*, 7854−7860.
(18) We have tested (U)M06-2X function for the present system and the results are not satisfactory (see SI for more discussions). Ess, D. H.; Cook, T. C. Unrestricted Prescriptions for Open-Shell Singlet Diradicals: Using Economical Ab Initio and Density Functional Theory to Calculate Singlet−Triplet Gaps and Bond Dissociation Curves. *J. Phys. Chem. A* **2012**, *116*, 4922−4929.
(19) (a) Bradley, A. Z.; Kociolek, M. G.; Johnson, R. P. Conformational Selectivity in the Diels-Alder Cycloaddition: Predictions for Reactions of s-trans-1, 3-Butadiene. *J. Org. Chem.* **2000**, *65*, 7134−7138. (b) Strickland, A. D.; Caldwell, R. A. Thermochemistry of strained cycloalkenes: experimental and computational studies. *J. Phys. Chem.* **1993**, *97*, 13394−13402. (c) Johnson, R. P.; DiRico, K. J. Ab Initio Conformational Analysis of trans-Cyclohexene. *J. Org. Chem.* **1995**, *60*, 1074−1076.
(20) Chen, K.; Wu, F.; Ye, L.; Tian, Z.-Y.; Yu, Z.-X.; Zhu, S. Cycloaddition Reaction of Vinylphenylfurans and Dimethyl Acetylenedicarboxylate to [8+2] Isomers via Tandem [4+2]/Diradical Alkene−Alkene Coupling/[1, 3]-H Shift Reactions: Experimental Exploration and DFT Understanding of Reaction Mechanisms. *J. Org. Chem.* **2016**, *81*, 8155−8168.
(21) (a) Strajbl, M.; Sham, Y. Y.; Villà, J.; Chu, Z.-T.; Warshel, A. Calculations of Activation Entropies of Chemical Reactions in Solution. *J. Phys. Chem. B* **2000**, *104*, 4578−4584. (b) Hermans, J.; Wang, L. Inclusion of Loss of Translational and Rotational Freedom in Theoretical Estimates of Free Energies of Binding. Application to a Complex of Benzene and Mutant T4 Lysozyme. *J. Am. Chem. Soc.* **1997**, *119*, 2707−2714. (c) Amzel, L. M. Loss of Translational Entropy in Binding, Folding, and Catalysis. *Proteins* **1997**, *28*, 144−149.
(22) Pohnert, G.; Boland, W. Pericyclic reactions in nature: Evidence for a spontaneous [1.7]-hydrogen shift and an 8πe electrocyclic ring closure in the biosynthesis of olefinic hydrocarbons from marine brown algae (phaeophyceae). *Tetrahedron* **1994**, *50*, 10235−10244.
(23) Timsina, Y. N.; Biswas, S.; RajanBabu, T. V. Chemoselective Reactions of (*E*)-1, 3-Dienes: Cobalt-Mediated Isomerization to (*Z*)-1, 3-Dienes and Reactions with Ethylene. *J. Am. Chem. Soc.* **2014**, *136*, 6215−6218.

https://dx.doi.org/10.1021/acs.joc.0c01960
J. Org. Chem. 2021, 86, 1419−1429